

Subjective Annotations for Vision-Based Attention Level Estimation

Andrea Coifman¹, Péter Rohoska^{1,3}, Miklas S. Kristoffersen^{1,2},
Sven E. Shepstone², and Zheng-Hua Tan¹

¹*Department of Electronic Systems, Aalborg University, Denmark*

²*Bang & Olufsen A/S, Struer, Denmark*

³*Continental Automotive, Budapest, Hungary**

Keywords: Attention Level Estimation, Natural HCI, Human Behavior Analysis, Subjective Annotations

Abstract: Attention level estimation systems have a high potential in many use cases, such as human-robot interaction, driver modeling and smart home systems, since being able to measure a person's attention level opens the possibility to natural interaction between humans and computers. The topic of estimating a human's visual focus of attention has been actively addressed recently in the field of HCI. However, most of these previous works do not consider attention as a subjective, cognitive attentive state. New research within the field also faces the problem of the lack of annotated datasets regarding attention level in a certain context. The novelty of our work is two-fold: First, we introduce a new annotation framework that tackles the subjective nature of attention level and use it to annotate more than 100,000 images with three attention levels and second, we introduce a novel method to estimate attention levels, relying purely on extracted geometric features from RGB and depth images, and evaluate it with a deep learning fusion framework. The system achieves an overall accuracy of 80.02%. Our framework and attention level annotations are made publicly available.

1 INTRODUCTION

Natural interaction has become an essential element in Human-Computer Interaction (HCI) over the past years. In the context of smart homes, the integration of intelligent systems into the home environment has improved the natural and effective communication between humans and home appliances. However, providing a natural interaction between smart devices and humans without the use of a physical device, e.g. a remote control, is still a challenging task. Vision-based systems are able to provide a more efficient and natural way of communication. As the years pass, these systems are starting to be more frequently applied into our daily living and homes. Although interaction between humans and computers is already well established in our homes, ways to make these systems more intelligent still draw much research interest. One common improvements is the integration of an intelligent system to give recommendations to the users (Gomez-Uribe and Hunt, 2016; Nararajavan and Govindarajan, 2016) based on learned interests. Most studies are based on integrating context-aware devices to track human behavior and routines

(Tamdee and Prasad, 2018). In this paper, we propose to use attention levels as an effective means to improve natural HCI in the home by measuring and classifying the attention level of a user. Attention can be defined as the focus of cognitive resources on a task, ignoring sources of distraction (Zaletelj and Košir, 2017). In other words, *attention is related to whether a user is focused or not on the task at hand, e.g. the interaction with a device.*

Quantitative techniques for measuring attention levels rely on the use of different sensors depending on the type of measurement: direct or indirect (Mancas and Ferrera, 2016). Direct measurements include brain responses e.g. by using EEG (Murthy G.N. and Khan, 2014) techniques, among others. However, extracting data from these sensors is expensive, intrusive, and uncomfortable for a natural communication. To address this problem, indirect measurement of attention levels has been studied through non-intrusive observation of users' behaviors, e.g. by using eye-trackers or head pose estimators (Asteriadis et al., 2011; Massé et al., 2017). Indirect measurements do not require the use of a physical sensor attached to the user, which makes the interaction with the system more natural. Most works on estimating attention levels through indirect measurements rely on the gaze direction of a user. This is due to the fact that the

*The presented work was done in affiliation with ¹ but the affiliation of the author changed to ³ during the submission.

eye gaze is highly correlated with what a user is interested in (Zaletelj and Košir, 2017). Existing datasets that provide annotations rely on objective frameworks e.g. calculating the direction of gaze or movements of eyes among other techniques (Kar and Corcoran, 2017).

This paper contributes to the field of HCI by providing subjective attention level annotations to an existing publicly available dataset, Pandora (Borghi et al., 2017), that contains visual recordings of users. A subjective label of attention level refers to the fact that each of the labelers bases their labeling decision on how they perceive each user’s attention level in the recordings, by taking the established definition of attention level into account. Based on the annotations, we further present a novel method that is able to measure attention level automatically. Our framework and attention level annotations are made publicly available². The remainder of this paper is organized as follows: Section 2 reviews previous state-of-the-art methods for estimating attention alongside existing datasets; Section 3 explains the process of annotating the dataset; Section 4 presents a baseline for estimating attention with subjective attention annotations; in Section 5 we present our experiments and quantitative results for the previously built baseline.

2 RELATED WORKS AND MOTIVATIONS

2.1 Vision-based Attention Estimation

First works on addressing attention estimation problems were based on predicting head pose or direction of eye gaze, which are considered to be high level descriptors of attention. This is due to the fact that, normally, the position of the head and the gaze direction are highly correlated with the subject of the user’s interest or, more applied to this paper, what caught the user’s attention (Jariwala et al., 2016; Zaletelj and Košir, 2017). Majority of studies focused on determining the Visual Focus of Attention (VFOA) for users’ attention estimation. The VFOA denotes the target of what a user is looking at and it is mostly determined by the combination of a user’s eye gaze and head pose dynamics (Massé et al., 2017). The VFOA characterizes a perceiver and target pair. It may be defined either by the line from the perceivers face to the perceived target, or by the perceivers direction of sight or gaze direction. However, estimating the attention level of a user based only on eye gaze can be

²<http://kom.aau.dk/~zt/online/SubjectiveAnnotations/>

problematic in the home context, due to the lack of detection range and the sensor’s low resolution.

In this work, we formulate the attention level estimation as a classification problem to be solved in a supervised learning framework, since we have subjective annotations of attention levels on a dataset. To this end, we propose a set of geometric features as an effective representation of high-level features that will serve as descriptors of the attention level of a user. The set of representative features consist of face, head, and body points, distances, and angles that describe the eye gaze direction together with head and body orientation of the user. There are a number of advantages of using the proposed features in a supervised framework. First, it includes more than eye gaze and pose information and thus is more descriptive. Second, it avoids deploying separate eye gaze and pose estimation systems and thus potentially reduces the complexity of the system. Finally, the system works even when eyes are not visible as multiple features are involved in the estimation of attention levels.

Many prior works in the field of HCI aim to use lower-level geometric features (e.g. locations, distances or angles between locations) to predict and classify higher-level features (e.g. direction of eye-gaze, body pose or head pose) for attention level estimation. Chen *et al.* (Chen et al., 2016) evaluated five dimensional feature vectors, containing geometric features of detected joints to evaluate joint motions for action recognition. Yun *et al.* (Yun et al., 2012) evaluates two-person interaction based on a wide variety of geometric body features, such as joint keypoints and distances, and joint-to-plane distances. Massé *et al.* (Massé et al., 2017) propose a framework where correlation between head pose and eye gaze is used to estimate the VFOA. The authors of some of these works also address the importance of these features to estimate attention in the field of HCI. To this extent, we decide to use geometric features and the corresponding relation between these features to evaluate the level of attention of a user.

2.2 Datasets and Annotation Methods

Different approaches have been proposed for generating attention estimation datasets and corresponding annotations. The most common way for researchers is to record their own datasets and hand label the images with information regarding the direction of the gaze (Tseng and Cheng, 2017) or shifts of attention between targets over the images in the dataset (Steil et al., 2018). All of the previously mentioned datasets and their annotations can be used to estimate the fo-

cus of attention, through the eye gaze and head pose labels. However, there are no existing information on the level of attention, even though, most of the datasets can be re-labeled with attention level annotations. Asteriadis *et al.* (Asteriadis et al., 2011) proposed a dataset similar to ours. In their work, the authors hand-labeled the Boston University (Boston, 2018) dataset using similar approaches regarding attention levels. First, the images were labeled regarding annotator’s perception of attention over the subject in the image, with two levels - ‘0’ and ‘1’ regarding attentive or non-attentive state. Second, an average decision rule was applied in order to evaluate the agreement between annotators. In contrast to the authors’ work, we hand-label the images with three levels of attention - ‘0’, ‘1’, and ‘2’ regarding low, medium, and high attentive state. For evaluating the level of agreement between annotators, we apply a “majority” decision rule which selects the final label as the one that has more than half of the votes from the labelers. In this way, we ensure a fair decision. Furthermore, we evaluate geometric features to address the problem of estimating attention level of a user.

3 SUBJECTIVE ANNOTATIONS

In this section, the publicly available dataset and the approach towards hand-labeling the 130,889 RGB images with subjective attention annotations are explained. A decision rule is later applied in order to evaluate the agreement between the labels from different labelers for each video frame.

3.1 Original Data and Reason of Use

Borghi *et al.* (Borghi et al., 2017) first introduced the Pandora dataset in 2016 as a part of research project in the automotive field for head center localization, head pose, and shoulder pose estimation. The dataset contains 110 sequences of 22 different subjects performing constrained and unconstrained driving-like movements. The data was collected using a Microsoft Kinect One device, which acquires the upper-body part of each of the subjects. The authors stated that, in this way, the position of the sensor would simulate as if it was located in the car’s dashboard. In this paper we follow this idea considering the lack of attention level datasets in the context of the living room. The position of the sensor and the captured upper-body simulates very well the idea of capturing attention level of a user from a smart system, such as smart TVs.

3.2 Annotation Method

In the present paper, a version³ of the dataset that contains 261,778 RGB (1920x1080 pixels) and depth (512x424) images was used. The dataset contains five different sequences of constrained (three) and unconstrained (two) actions from 20 different subjects. Contrary to previous datasets explained in Section 2.2 with annotations based on shifts of attention, we propose a frame-by-frame approach, in order to better understand the context and different situations. To this end, the data was re-structured as unique sequences for each of the 20 subjects, with jointly constrained and unconstrained movements, ending up with an average of 6,544 RGB frame images per subject. The frames were manually annotated with subjective annotations of attention level by five annotators: four were used for labeling and one for checking. A subjective label of attention level refers to the fact that each of the labelers based their labeling decision on their personal feelings and opinion. An objective definition of attention (see Section 1) was provided to the labelers beforehand, along with the definition of each attention level:

- ‘0’ Low attention level: The subject was not paying attention to the task at hand.
- ‘1’ Mid attention level: The subject was partially paying attention to the task at hand.
- ‘2’ High attention level: The subject was paying full attention to the task at hand.

3.3 Decision Rule and Agreement

The total number of annotations was 523.556 (four labels per frame). In order to measure the agreement between the annotators, a decision rule was determined. In this way, every frame would have a unique label. The decision rule aim to assign the most fair label to each of the frames. A first decision rule was applied over the annotations by selecting the alternative that had more than half of the votes (majority rule). In this way, votes were treated equally. Having four annotations per frame, majority was settled when three or more labels were equal, ending up with an agreement over all the annotations from the dataset of 79.7%. In order to increase the percentage of agreement between the annotators, a checker labeler was introduced to annotate the unsolved frames. The annotations procedure for the checker was the same as for the rest of the annotators (explained in Section

³The authors are still updating the Pandora dataset with new RGB and depth images. Last noticed version updated on 29th of May, 2018.

3.2). After the checker annotated the frames, a second majority decision rule was applied over each five annotations per frame. The resolved labels between annotators increased to 92.6% of the frames. A median filter was applied to decide the label for the remaining frames.

The distribution of the annotations in the dataset is as follows: the labels corresponding to low attention level occupy most of the labeled data with 70.8% of annotations; mid and high attention level annotations are more or less equally distributed with a total of 15.5% and 13.7% of annotations over the total labeled dataset, respectively. Table 1 shows the number of frames and the agreement between annotators before and after integrating the checker, for each subject or set of images. Fig. 1 shows an example of three different frames extracted from the Pandora dataset with their corresponding final label of level of attention, after the agreement between annotators: Fig. 1a shows a subject manipulating a second screen, representing subjective low level of attention; Fig. 1b shows a subject which head position is not aligned with the direction of the gaze, representing the subjective medium attention level (mid); and Fig. 1c shows a subject looking directly to the sensor, which clearly represents the subjective high attention level.

4 ATTENTION LEVEL ESTIMATION METHODS

In this section, we first introduce the proposed features and methods for attention level estimation. First, we explain the procedure for extracting the keypoints, we define the geometric features and present our approach to integrate depth. And second, we explain three simple machine learning methods and five complex deep learning models.

4.1 Feature Extraction

All keypoint coordinates are extracted using the publicly available OpenPose API (Hidalgo et al., 2018) from the RGB images of the annotated dataset. We use RGB color space since the original OpenPose model was trained using the same color space. For addressing the problem of attention estimation, we extract keypoints representing body and face parts of the user. Neck and right/left shoulder keypoints are extracted for describing the upper-body of the subject. Nose and eye center keypoints for the right and left eye are extracted for describing the face of the subject, and six eye contour keypoints for describing the

right/left eyes. In cases when the API outputs multiple people for only one person (e.g. either a false positive detection or breaking the keypoints of one person into two), we find the similarity between two keypoint vectors and merge them if the missing keypoints are correlated. Since some of the keypoints from various frames can still be missing after this operation, we interpolate between the last detection and the most recent detection, for each keypoint, to create a continuous stream of detections.

Before constructing our geometric features described below, we recalculate the position of each keypoint on each frame according to the coordinate system where the nose keypoint represents the origin. This way we can transform our features from being relative to the image coordinate system and instead construct them localized.

The geometric features were inspired by Zhang *et al.* (Zhang et al., 2018) and are constructed based on the extracted keypoints. They consist of a set of relations between keypoints. Two types of geometric features were defined:

1. A set, D , of Euclidean distances between keypoints.
2. A set, A , of angles between two unit vectors, each of which represents a line linking two consecutive keypoints.

The first set of geometric features is described by four types of distances:

$$D = \{D_F, D_{BF}, D_{LE}, D_{RE}\}, \quad (1)$$

where D_F corresponds to the Euclidean distances between face keypoints and is defined by:

$$D_F = \{\|\mathbf{f}_j - \mathbf{f}_i\| \mid i, j \in F, i < j\}, \quad (2)$$

with F being the face keypoints, and \mathbf{f}_i the coordinate of the i^{th} face keypoint. D_{BF} corresponds to the Euclidean distances between face and body keypoints and is defined by:

$$D_{BF} = \{\|\mathbf{f}_j - \mathbf{b}_i\| \mid i \in B, j \in F\}, \quad (3)$$

where B are the body keypoints and \mathbf{b}_i the coordinate of the i^{th} body keypoint. D_{LE} corresponds to the Euclidean distances between left eye center keypoint to each six contour keypoints of the left eye and they are defined by:

$$D_{LE} = \{\|\mathbf{e}_i - \mathbf{c}_L\| \mid i \in LE\}, \quad (4)$$

with LE being the contour keypoints of the left eye, \mathbf{e}_i the coordinate of the i^{th} contour keypoint, and \mathbf{c}_L the coordinate of the left eye center. Similarly, D_{RE} corresponds to the Euclidean distances between right eye center keypoint to each six contour keypoints of the right eye.

Table 1: Agreement between annotators and checker for the annotated dataset

Set #	1	2	3	4	5	6	7	8	9	10	11	12	13	14	15	16	17	18	19	20	Mean	Std
# Frames	5197	5562	6317	6706	5340	6222	4861	6907	6433	6757	5295	6820	7312	8122	7396	6014	7130	8976	8689	4833	-	-
% Majority settled between annotators	94.15	83.75	78.12	68.92	82.02	65.67	81.98	80.32	92.04	91.86	64.49	76.73	83.52	74.17	82.18	76.02	86.94	65.66	88.20	80.96	79.89	8.8245
% Majority settled with checker	98.19	94.70	90.87	85.71	94.14	85.26	95.23	94.90	98.91	97.60	82.85	90.62	93.34	93.70	92.39	91.57	96.06	87.32	96.05	92.72	92.61	4.2085

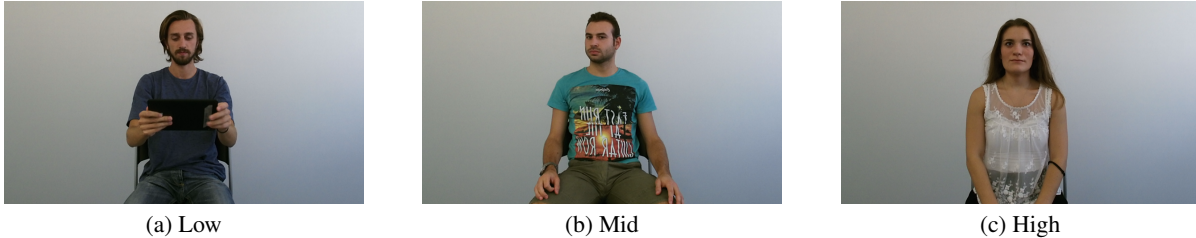
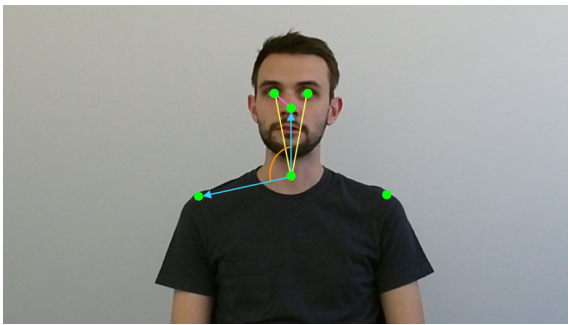


Figure 1: Example of frames with the corresponding three label of attention level.

Figure 2: Graphical representation of keypoints and geometric features in colors: green for keypoints, pink for D_F , yellow for D_{BF} , blue for vectors used to compute the angles (orange). Original image extracted from Pandora dataset (Borghini et al., 2017).

For the definition of the set, A , we compute three unit vectors. One between nose and neck:

$$\mathbf{v}_1 = \frac{\mathbf{f}_{nose} - \mathbf{b}_{neck}}{\|\mathbf{f}_{nose} - \mathbf{b}_{neck}\|}. \quad (5)$$

And two between neck and left/right shoulders, respectively:

$$\mathbf{v}_2 = \frac{\mathbf{b}_{Lshoulder} - \mathbf{b}_{neck}}{\|\mathbf{b}_{Lshoulder} - \mathbf{b}_{neck}\|}, \mathbf{v}_3 = \frac{\mathbf{b}_{Rshoulder} - \mathbf{b}_{neck}}{\|\mathbf{b}_{Rshoulder} - \mathbf{b}_{neck}\|}. \quad (6)$$

We then describe the set as:

$$A = \{\arccos(\mathbf{v}_1^T \mathbf{v}_2), \arccos(\mathbf{v}_1^T \mathbf{v}_3)\}, \quad (7)$$

which are two angles between neck to nose vector and vectors from neck to left/right shoulders, respectively.

Research within computer vision has shown that, in many applications, when depth information is included along with RGB imagery, the extra modality can improve the performance of the system (Li and Jarvis, 2009; Molina et al., 2015). We extract depth information on a point of interest basis. This process covers finding positions on the original RGB image,

where depth information is to be extracted using the already computed keypoints as keys. By taking the average depth in a 3×3 area around each position, we alleviate the problem of possible small positional errors in the extracted keypoints. Note that the extraction of depth pixel intensity information is done after interpolating the missing keypoint coordinates, but before recalculating the keypoint coordinates according to the Nose keypoint. Once all features are extracted, we standardize them.

4.2 Attention Level Estimation

In this section, we present several methods for attention estimation with subjective attention annotations, which can serve as baselines for further development. We use our own baseline for attention level estimation, since we find that there are no adequate baselines at the present and we consider our novel attention level estimation framework and subjective labeling process a pioneer work.

Before training DNN models for attention level classification, we train and evaluate three classic machine learning models, to set up a baseline for our more complex models performance. We train Support Vector Machine (SVM), Logistic Regression (Logit) and a single hidden layer Multilayer Perceptron (MLP) for multiclass classification.

4.2.1 Deep Neural Network (DNN) Models

Using all of our feature space as a whole, as the input to our DNN models (“early” fusion, see Fig. 3a), might not always yield the best possible result. Other studies made their efforts on fusing multiple keypoints and geometric features (Zhang et al., 2018), and argue that fusing these features together at a later stage of the network - either by training a fully con-

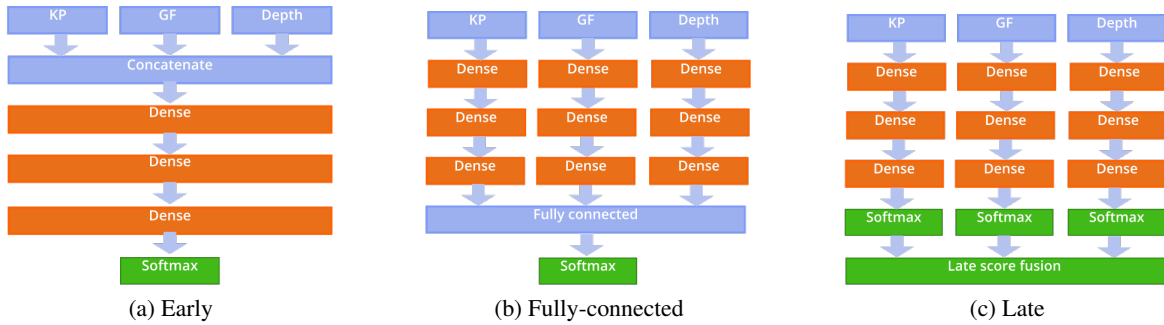


Figure 3: DNN models and methods for fusing keypoints (KP), geometric features (GF) and depth.

nected layer on top of different dense layer streams (“fully-connected” fusion, see Fig. 3b) or combining the softmax decisions (“late” fusion, see Fig. 3c) - can further increase the overall classification accuracy. To further evaluate our extracted features, we decided to follow the three feature fusion frameworks, explained below. Note that in all models where we apply fully-connected or late fusion, we handle keypoints, geometric features and/or depth in streams of separate dense layers. Further on, in this paper, these streams are noted as *feature streams*.

Early fusion: the keypoints and geometric features (when having two modalities) and depth (three modalities) are concatenated and given as input to the DNN models during training and inference.

Fully-connected feature fusion: the degree of how much each feature subset contributes to the classification task at hand is learned through different information streams based on the input. This is possible to be learned through trainable weights of a DNN. Each stream represents layers of densely connected neurons that are kept separately for each stream and are only connected to a fully connected layer at a later stage, before classification. This way the different layers of each stream can learn unbiased information by the other stream, but share information through the neurons of the fully connected layer, before classification.

Late fusion: this approach integrates common meaning representations derived from different modalities into a combined final interpretation, by utilizing separate classifiers that can be trained independently. The final decision is reached by combining the partial outputs of the unimodal classifiers, by either taking the maximum (maximum fusion) or the average scores of all feature stream specific softmax layers (average fusion) train a set of learnable weights on top of each softmax layer and attaching a new softmax layer on top of these weights, to reach the final classification scores (Kuang et al., 2016).

Each of the dense layers have 256 and fully con-

nected layers have 64 hidden units, with ReLU activations. The learning rate was initially set to 0.0001 for the Adam optimizer. In case of fully-connected fusion and weighted score fusion, we train the different feature streams separately. When we train the fully connected fusion models, the softmax layers of each stream are detached and connected to a fully connected layer which is further connected to its own softmax layer. We freeze the weights of each feature stream and only update the weights of the new layers during backpropagation. With this procedure, we can deny the bias in each stream caused by the parallel ones. We train our late fusion models in the same fashion, except we keep the softmax layers, and attach a new custom layer that operated on the decision of each stream.

5 EXPERIMENTAL RESULTS AND DISCUSSION

Four-fold cross-validation were used for evaluating the presented algorithms. The final accuracy is obtained as the average of all the accuracies of all four models from each algorithm. Table 2 shows the performance of the classic machine learning algorithms over the dataset alongside the performance of the different DNN models for each modality in terms of accuracy.

From our experiments, we find that including depth information among the input features is mostly beneficial. Table 2 shows that both the early and fully-connected fusion of keypoints, geometric features and depth outperforms the fusion of keypoints and geometric features. The three different versions of late fusion models did only make a marginal difference between the same results. From the results of our best performing model (fully-connected fusion with three modalities, see Table 2) we find that most false negative and false positive classifications

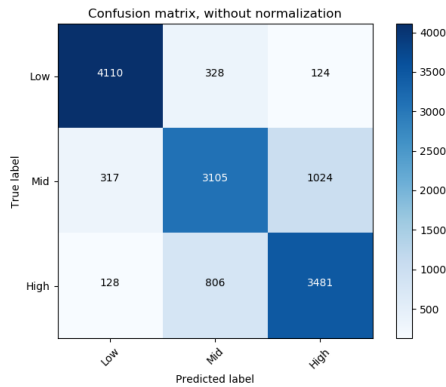


Figure 4: Confusion matrix of the results of the fully-connected fusion of keypoints, geometric features and depth. Darker colors correspond to a larger number of classifications.

are performed regarding “mid” attention level. Fig. 4 shows that more than 60% of the false classifications happen along the “mid” label. This result can be best explained by the nature of the annotations. Although in most cases “low” and “high” attention level was clearly decided by the majority votes of the annotators, “mid” attention level was mostly decided by the final agreement rule or the checker’s annotations. This meant that most images which caused confusion or a difficult decision for the annotators fell under the “mid” attention label, resulting in the most difficult and versatile class of all three. It is also important to note that when one of the DNN models outperformed a previous one, the performance change was best visible on the misclassification rate of the “mid” class.

The results in Table 3 show how accurately individual streams estimate single attention level classes (accuracy per individual class label). It is clearly visible that keypoints perform the estimation of low and mid attention level the most accurate, however geometric features are the best at estimating high attention level. Although depth is an overall low accuracy descriptor of attention, the results from Table 2 justify

Table 2: Performance of the classic algorithms and DNN models with two (KP and GF) and three (KP, GF and depth) modalities.

Model		Accuracy	Standard deviation	
SVM		0.6121	0.0043	
Logit		0.5887	0.0030	
MLP		0.6314	0.0155	
Early fusion	KP + GF	0.7293	(0.0020-0.0040)	
	KP + GF + Depth	0.7547		
Fully-connected fusion	KP + GF	0.7781		
	KP + GF + Depth	0.8002		
Late fusion	Average	KP + GP		0.7196
		KP + GF + Depth		0.7169
	Maximum	KP + GF		0.7161
		KP + GF + Depth		0.7075
	Weighted	KP + GF		0.7236
		KP + GF + Depth		0.7234

Table 3: Results of how accurately individual streams estimate single attention level classes (accuracy per individual class label).

	Accuracy per individual class label		
	Low	Mid	High
Keypoints	0.8938	0.7470	0.7807
Geometric Features	0.8909	0.7434	0.7886
Depth	0.7764	0.6704	0.6745

the inclusion of depth information. These results show fusion (on any level) of different modalities can help to increase the model’s overall performance for the task at hand. Table 2 shows that late fusion’s performance was always inferior compared to the other two versions of fusion. This is best explained by late fusion only being a powerful tool when it is introduced to modalities that are represented differently in the input data. This difference can refer to difference in temporal aspects or representation (e.g images and numeric data or sound). Neither of the feature subsets and modalities that were fused together differ on a temporal aspect and the way these features or modalities are represented in the feature space, which explains the inferior performance of all late fusion models. To validate these results, we introduced a new fusion model, where the geometric features were fused together in a fully-connected model, and fused together with the depth features in a weighted late fusion model. The results of the new fusion can not over perform the results of the best fully connected fusion model either. The better performance of the fully connected fusion model can be best explained by the nature of the method. Since all streams are kept separated for the early stages of the network, the learned weights inside the stream specific layers are less correlated to each of the fusion streams. However, the classification error is propagated back to each of these layers, during global optimization. Therefore, the model can still adjust its learned parameters according to the other separated streams. This way, the learned information is only limited throughout the early stages of training.

6 CONCLUSION

Estimating attention level of a user is a very challenging task. The majority of methods rely on describing attention by measuring the VFOA of a user with combination of head pose estimation. The development of datasets in the field have been at the focus point in research over the past years. However, existing datasets either do not include annotations or rely on objective annotations depending on the direc-

tion of the eye gaze and head pose of a user. In this paper, we proposed a novel approach towards estimating attention level of a user with subjective annotation levels by evaluating geometric features. We hand-labeled over 100,000 images of the Pandora dataset with three levels of subjective annotations, using five participants. The objective of the labeling process was to label attention level of data based solely on personal feelings and opinion, which we believe is beneficial for tasks such as estimating the attention level of a user, to incorporate the subjective nature of attention itself. We further set up baseline results of attention level estimation, using our annotations and different deep learning fusion models. Our best achieved accuracy was 80.02% on attention level estimation. As a future work, we consider labeling the dataset for other applications in the field related to attention, such as the VFOA (looking at the TV or not) of each person, frame-by-frame. Shift of attention labels can also be added, e.g annotating the frames where the attention shifts from low to mid, mid to high and high to low.

REFERENCES

- Asteriadis, S., Karpouzis, K., and Kollias, S. (2011). The Importance of Eye Gaze and Head Pose to Estimating Levels of Attention. *2011 Third International Conference on Games and Virtual Worlds for Serious Applications*.
- Borghì, G., Venturelli, M., Vezzani, R., and Cucchiara, R. (2017). POSEidon: Face-from-Depth for Driver Pose Estimation. *IEEE Conference on Computer Vision and Pattern Recognition*.
- Boston, U. (2018). Boston university common data set 2017-2018.
- Chen, H., Wang, G., Xue, J.-H., and He, L. (2016). A novel hierarchical framework for human action recognition. *Pattern Recognition*, 55:148–159.
- Gomez-Uribe, C. A. and Hunt, N. (2016). The Netflix Recommender System: Algorithms, Business Value, and Innovation. *ACM Transactions on Management Information Systems*, 6(4):Article No. 13.
- Hidalgo, G., Cao, Z., Simon, T., Wei, S.-E., and Joo, H. (2018). OpenPose: Real-time multi-person keypoint detection library for body, face, and hands estimation. original-date: 2017-04-24T14:06:31Z.
- Jariwala, K., Dalal, U., and Vincent, A. (2016). A robust eye gaze estimation using geometric eye features. *Third International Conference on Digital Information Processing, Data Mining, and Wireless Communications*.
- Kar, A. and Corcoran, P. (2017). A Review and Analysis of Eye-Gaze Estimation Systems, Algorithms and Performance Evaluation Methods in Consumer Platforms. *IEEE Access*, 5:16495–16519.
- Kuang, H., Chan, L. L. H., Liu, C., and Yan, H. (2016). Fruit classification based on weighted score-level feature fusion. *Journal of Electronic Imaging*, 25(1).
- Li, Z. and Jarvis, R. (2009). Real time Hand Gesture Recognition using a Range Camera. *Australasian Conference on Robotics and Automation (ACRA)*.
- Mancas, M. and Ferrera, V. (2016). How to Measure Attention? *Mancas M., Ferrera V., Riche N., Taylor J. (eds) From Human Attention to Computational Attention*, 10.
- Massé, B., Ba, S., and Horaud, R. (2017). Tracking Gaze and Visual Focus of Attention of People Involved in Social Interaction. *Computing Research Repository*, Computer Science(Computer Vision and Pattern Recognition).
- Molina, J., Pajuelo, J. A., and Martínez, J. M. (2015). Real-time Motion-based Hand Gestures Recognition from Time-of-Flight Video. *Springer Science+Business Media New York 2015*.
- Murthy G.N., K. and Khan, Z. A. (2014). Cognitive attention behaviour detection systems using Electroencephalograph (EEG) signals. *Research Journal of Pharmacy and Technology*, 7(2):238–247.
- Nararajasivan, D. and Govindarajan, M. (2016). Location Based Context Aware user Interface Recommendation System. *Proceedings of the International Conference on Informatics and Analytics*, page Article No. 78.
- Steil, J., Müller, P., Sugano, Y., and Bulling, A. (2018). Forecasting user attention during everyday mobile interactions using device-integrated and wearable sensors. *Proceedings of the 20th International Conference on Human-Computer Interaction with Mobile Devices and Services*.
- Tamdee, P. and Prasad, R. (2018). Context-Aware Communication and Computing: Applications for Smart Environment. *Springer Series in Wireless Technology*.
- Tseng, C.-H. and Cheng, Y.-H. (2017). A camera-based attention level assessment tool designed for classroom usage. *The Journal of Supercomputing*, pages 1–14.
- Yun, K., Honorio, J., Chattopadhyay, D., Berg, T. L., and Samaras, D. (2012). Two-person interaction detection using body-pose features and multiple instance learning. *IEEE Computer Society Conference on Computer Vision and Pattern Recognition Workshops*.
- Zaletelj, J. and Košir, A. (2017). Predicting students' attention in the classroom from Kinect facial and body features. *EURASIP Journal on Image and Video Processing*, 2017(80).
- Zhang, S., Yang, Y., Xiao, J., Liu, X., Yang, Y., Xie, D., and Zhuang, Y. (2018). Fusing Geometric Features for Skeleton Based Action Recognition using Multilayer LSTM Networks. *IEEE Transactions on Multimedia*, 20(9).